Accelerating Power Flow Simulations
Using Function Mapping

Michael Bardwell[*], Petr Musilek[*][†]

[*]Department of Electrical and Computer Engineering, University of Alberta, Edmonton, AB, Canada
[†]Department of Cybernetics, Faculty of Science, University of Hradec Králové, Czech Republic

Abstract—The main contributions of this paper include demonstrating the function approximation of the power system load flow (PSLF) function. A hyperparameter grid search was used to confirm the optimal training conditions. It was discovered that for large radial networks, the identity linear regression outperforms non-linear regression. This indicates PSLF is a relatively linear function even when the feature space is large. The author's developed a Python-based framework to autonomously handle simulation function mapping.

I. INTRODUCTION

Modern simulation techniques are expensive. High resolution, complex simulations can take on the order of hours or days to come to completion and require advanced, costly computers. When these simulations are completed, it is likely the researcher or practitioner will run another, restarting the whole process. The institutional solution is to purchase faster, more expensive computers. While the outputs of the simulation are the desired results, no conclusive research has been done on capturing the simulation model for re-use. It is viewed as a black box, often deleted post-simulation only for the same model to be rerun later on a different input sequence.

Today's simulation models are handled in engines like MATLAB Simulink, which are highly multivariate, nonlinear equations, masked by a graphical user interface and solved using numerical methods. Advanced regression techniques and computing power has made it possible to capture extremely high-dimensional, nonlinear systems of equations. This paper explores the regression techniques successful in function approximating the topological correspondence in electric power grids.

The general regression formula is shown in eqn (1). The function is linear with respect to the weights w, and the basis functions $\phi(x)$. One-layer artificial neural networks is an example of an estimator consistent with this formula and will be discussed further in this paper.

$$f(x) = \sum_{i=0}^{z} w_i^T \cdot \phi_i(x) \qquad (1)$$

The electric power grid is governed by the power system load flow (PSLF) equation in eqn (2). PSLF defines the relationship between the input power vector S_i, and the output voltage vector $V_{i/k}$. The user creates a Y-bus admittance matrix $Y_{ii/ik}$ by selecting the bus connection topology like the radial topology in Fig. 1, where each circle represents a house. Our focus is to capture the unique correspondence between houses using function mapping.

$$V_i = \frac{1}{Y_{ii}} \cdot \left(\frac{S_i^*}{V_i^*} - \sum_{k=1, k \neq i}^{n} Y_{ik} \cdot V_k \right) \qquad (2)$$
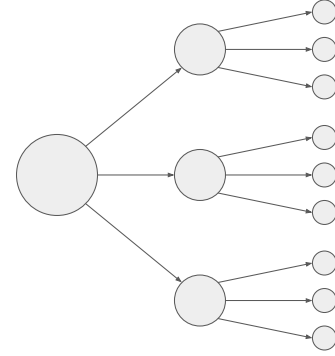

Fig. 1. A sample radial network

There are many function approximation techniques, starting in statistics with methods like nonlinear least squares and maximum likelihood estimates which belong to a broader class called M-estimators [1]. Radial basis functions are used in [2] to model nonlinear voiced speech sounds. Chen develops a backpropagation technique for multi-layer perceptron function approximation in [3]. Similarly, techniques such as wavelets [4], kernal-type methods [5] and projection pursuit models [6] all provide nonlinear approximations. [7] develops the concepts of extrema equivalence to estimate the complexity of a function, thereby providing an empirical method to select ANN network size and toplogy. [8] provides a statistical perspective on many of the aforementioned techniques; for example, assuming $f(x)/V$ is inside the convex hull of a trained one-layer ANN represented as f_M, amongst a few other assumptions, we can say the approximation error is bounded as:

$$\|f - f_M\| \leqslant \frac{V}{\sqrt{M}} \qquad (3)$$

Where M is the number of neurons in the hidden layer.

Artificial neural networks (ANN) are a good choice for function approximation due to their adjustable basis function

nature [9], this is excellent for our application as there is uncertainty in the nature of the PSLF-based function to be approximated, so adjustable basis functions will make development easier.

Once a function has been approximated, it is important to make it as usable as possible. A Python program was developed to autonomously handle the PSLF function approximating. The program is summarized in Fig. 2.

In Section II the nuances of function approximating are discussed. In Section III the experimental method is outlined, and then the method is executed and results tabulated in Section IV. Section V summarizes the contributions of this paper. The research is wrapped in an open-source Python package available through *pip install simhandler* or GitHub[1].

II. BACKGROUND

A mapping is a rule of correspondence between input and output vectors. To function map a simulation model, two sets of vectors $a_i \in R^p$, $b_i \in R^q$ are required: a finite input data set $\{a_0, a_1, \ldots, a_m\}$ and a finite output data set $\{b_0, b_1, \ldots, b_n\}$; the output set is calculated by passing the input set through a well-defined simulation model. m, n are the number of input/output features in the simulation model respectively and the length of each vector in either set is defined as the number of samples and is orthogonal to m, n. For example, an MNIST identifier might have an m = 1000, n = 10 reflecting 1000 pixels per image and 10 possible outcomes (digits 0-9) respectively.

The more non-linear the simulation model, the more samples required for function mapping to meet high accuracy goals. For example, imagine the simulation model is a simple, two-dimensional linear function. From eqn (1), assuming $\phi(x) = \{1, x\}$

$$f(x) = w_0 + w_1 \cdot x \tag{4}$$

To determine the bias w_0 and weight w_1, you only require two, linearly independent, m-dimensional data points. Now imagine a more likely scenario for a simulation model, which produces a noisy function like in Fig. 3.
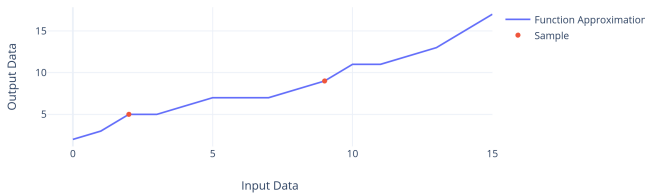

Fig. 3. Sample simulation data

It is obvious by inspection that any line, like one drawn between the two sample dots in Fig. 3, would be an underfitted

[1]https://github.com/mbardwell/intelligent-simulation-handler

approximation of the correspondence in this simulation. The underfitting is exponentially amplified in higher dimensions, due to the curse of dimensionality. For parameterized models, much more data is required to get a better approximation of the relationship encoded in a simulation.

To map the PSLF equation, a feed-forward ANN with rectified linear units (ReLU) is fed electric power system data. Pre-processing for this data is minimal as each feature is already geometrically balanced; also using per unit ensures the input/output values are close to 1. The network is trained using simple backpropagation. A Monte Carlo approach is taken to fill S_i using a uniform distribution with support $x \in [0, 1)$; the stochastic approach optimizes the efficiency of mapping nonlinear functions, much like random search optimizes efficiency for hyperparameter exploration[10].

There are many variations in power system topology, see Table I. The objective in this paper is to provide the experimental procedure for function mapping a radial feeder network with resistive-only lines. The methodology should naturally extend to other variations as well. It is important to note that to a power-system engineer, an accuracy of 10^{-2} is good enough. For example, if the base voltage for a distribution line is 35 kV, the upper bound on the estimation error would be 350 V.

PS Parameter	Examples
Bus Topology	Main-Tie-Main, Ring, Primary Loop
Feeder Network	Radial, Parallel, Ring, Meshed
Line Characteristics	Resistance, Reactance, Length, Maximum Power
Line Support	Shunt/Series Compensation
Storage Parameters	BESS's, Flywheels, Compressed Air
Generator Availability	Minimum/Maximum Real and Reactive Power

TABLE I
POWER SYSTEM NETWORK PARAMETERS

Mean-square error (MSE), also known as the L_2 or Euclidean norm is the accuracy metric used for ANN training. It is optimal for function approximation as it is more sensitive to outliers than mean absolute error. Root-MSE (RMSE) will be used for analysis, however, since it is in the same units as the feature space.

To demonstrate the accuracy capabilities of nonlinear function mapping, the results are compared to an identity linear regression (ILR) with m-dimensions, which is derived by setting $\phi_i(x) = x_i$ in eqn (1).

$$f(x) = w_0 + \sum_{i=1}^{m} w_i^T \cdot x_i \tag{5}$$

For smaller-featured systems, ILR may out-perform the ANN. This is because PSLF with very small systems tends to have little noise; also ILR is fitted to the data, which unlike gradient descent used in ANN training is an exact process. ILR is fitted using the normal equation.

$$\hat{\theta} = (\mathbf{X}^T \cdot \mathbf{X})^{-1} \cdot X^T \cdot \mathbf{y} \tag{6}$$

One non-obvious trade off between ILR and ANN is the expensive nature of normal equation calculations; for ILR a matrix inversion is required, which in Big-O notation is
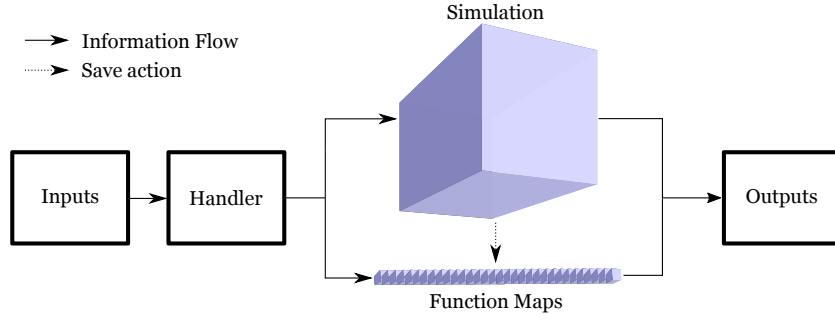
Fig. 2. Flow of information in Simulation Handler Python program. The user provides a simulation model and input samples and the handler automates the PSLF process. The output is a set of node voltages concurrent with the samples seen at the input

between $O(m^{2.4}) - O(m^3)$. ANN training scales linearly, or $O(m)$. This is demonstrated by the timing comparison in Fig. 4.
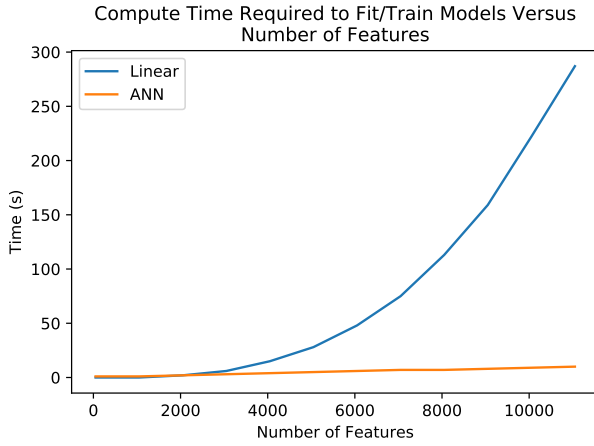

Fig. 4. Compute time required to fit an ILR (*Linear* in legend) using the normal equation versus train an ANN using backpropagation

III. EXPERIMENTAL METHOD

The generic approach to function approximating PSLF equations is outlined in Fig. 5. To achieve results in swift fashion, a hyperparameter search will be automated using an open-source Python library, Talos.
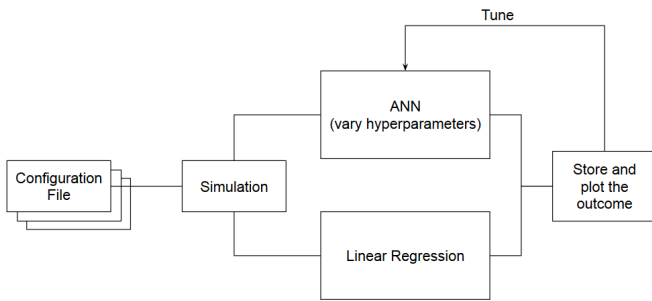

Fig. 5. General approach to function mapping PSLF equations

According to [3][11], three-layer ANN's are considered universal approximators. Naturally, this would be a good starting number of hidden layers, however preliminary tuning with ILR's which are similar to one-layer ANN's has shown reasonable results, so the number of hidden layers will be tuned between 1-3.

Sample size is also important. Since a Monte Carlo approach is taken to fill S_i, a theoretical infinite number of samples could be used to fit/train the approximation. This is unrealistic, so a preliminary study was done to determine the time it takes to calculate the outputs from the iterative PSLF process. Note the intention of this study is to observe the extremums of accuracy, so a high sample/small feature space approach was taken.
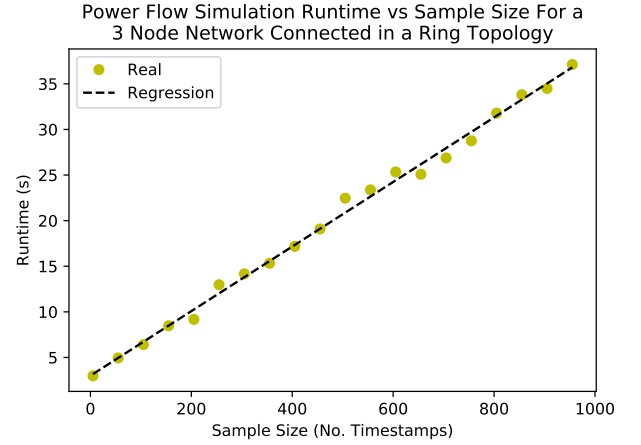

Fig. 6. Power system load flow analysis time requirements as a function of sample size. Run on Intel Core i5 and 16 GB of RAM

The results from Fig. 6 show the runtime increases around $0.034\ s/sample$ for a very small network. Another study showed an increase of $0.016\ s/feature$. This gives us the following runtime equation: $t(s) = 0.034 \cdot N + 0.016 \cdot m$, with N being the number of samples. The study will be capped at m = 200 and N = 5 000 which puts our maximum runtime around 3 minutes, which is very reasonable as it allows us to collect many data points. In short, N will be bound by $[m_{min}, 25 \cdot m]$. The optimization algorithm will be ADAM, a very popular variant of momentum-based optimizers and the initial learning rate will be set to 10^{-4}.

IV. Results

Using 100 samples, a grid search was performed on a simple 3 node, radial network. The validation loss in Fig. 7 shows that sigmoid performs about 4 times better on average than ReLu. Layer density appeared to have the next biggest effect, followed by number of layers. Initial learning rate had an unnoticeable effect.

mae	mse	val_mae	val_mse	val_rmse	first_neuron	lr	hidden_layers	Activation
3.96E-03	8.12E-05	4.46E-03	1.17E-04	1.08E-02	16	1.00E-05	1	relu
4.41E-03	3.21E-05	6.22E-03	6.76E-05	8.22E-03	64	0.001	1	relu
5.22E-03	6.80E-05	7.72E-03	1.49E-04	1.22E-02	32	1.00E-05	1	relu
2.80E-03	1.83E-05	4.50E-03	7.97E-05	8.93E-03	16	0.001	1	relu
3.52E-03	2.02E-05	6.17E-03	7.00E-05	8.37E-03	64	1.00E-05	1	relu
9.06E-03	1.32E-04	1.22E-02	2.32E-04	1.52E-02	32	0.001	1	relu
2.90E-03	1.64E-05	4.64E-03	5.12E-05	7.16E-03	64	0.001	3	relu
4.80E-03	6.00E-05	6.39E-03	1.30E-04	1.14E-02	16	0.001	3	relu
6.45E-03	7.79E-05	7.37E-03	9.60E-05	9.80E-03	32	1.00E-05	3	relu
1.14E-02	2.05E-04	1.16E-02	2.14E-04	1.46E-02	16	1.00E-05	3	relu
4.33E-03	2.82E-05	7.90E-03	1.23E-04	1.11E-02	64	1.00E-05	3	relu
6.83E-03	8.79E-05	6.95E-03	8.18E-05	9.04E-03	32	0.001	3	relu
				1.06E-02				
1.04E-03	1.83E-05	9.77E-04	2.03E-06	1.43E-03	64	0.001	1	sigmoid
5.13E-05	6.55E-05	4.28E-03	3.78E-05	6.15E-03	16	1.00E-05	1	sigmoid
6.66E-04	1.09E-06	7.30E-04	1.20E-06	1.09E-03	64	1.00E-05	1	sigmoid
3.35E-03	2.44E-05	3.42E-03	2.25E-05	4.74E-03	16	0.001	1	sigmoid
1.51E-03	3.97E-06	1.53E-03	4.27E-06	2.07E-03	32	0.001	1	sigmoid
1.25E-03	2.87E-06	1.32E-03	3.34E-06	1.83E-03	32	1.00E-05	1	sigmoid
2.48E-03	1.38E-05	2.31E-03	1.09E-05	3.30E-03	16	1.00E-05	3	sigmoid
2.98E-03	1.48E-05	2.71E-03	1.20E-05	3.46E-03	16	0.001	3	sigmoid
1.49E-03	4.58E-06	1.63E-03	5.76E-06	2.40E-03	32	0.001	3	sigmoid
1.11E-03	2.18E-06	1.18E-03	2.16E-06	1.47E-03	32	1.00E-05	3	sigmoid
6.02E-04	6.80E-07	5.59E-04	5.42E-07	7.36E-04	64	0.001	3	sigmoid
5.94E-04	6.28E-07	5.38E-04	5.49E-07	7.41E-04	64	1.00E-05	3	sigmoid
				2.45E-03				

Fig. 7. Grid search. Manipulated Hyperparameters include activation function, number of layers, density of layers, learning rate. Activation function had the largest effect as expected

Fig. 8 shows the results of function approximating with ILR. It's clear that when the sample-to-feature ratio approaches two, the error exponentially ramps upwards. It can also be observed that for sample-to-feature ratios above five, the results are very similar. This suggests that there is a statistically significant sample-to-feature roof for ILR around 5, which permits an empirical selection of samples when given the number of features by the user.
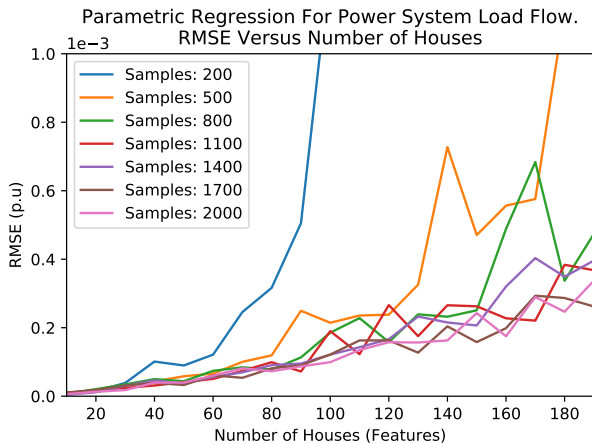

Fig. 8. ILR for PSLF equations with various input features spaces and sample

The results in Fig. 9 show that the nonlinear ANN solution produces more error than the ILR fit. This would suggest that the PSLF has very little noise, even when the feature space is as large as 200 dimensions. Further hyperparameter tuning is required as this results is illogical. One interesting observation from the figure is the approximation results are much more sporadic when the samples-to-feature ratio is below 5 confirming the nonlinear solution requires more data than the ILR to be trained to a low RMSE.
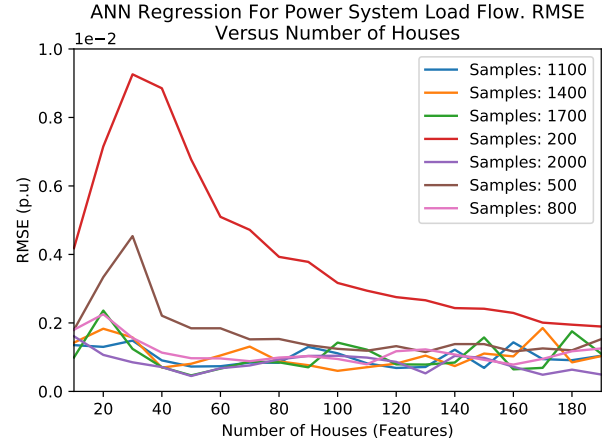

Fig. 9. ANN for PSLF equations with various input features spaces and samples

Fig. 10 visualises the accuracy of function approximating with both ILR and ANN mappings for one node in a 500 house radial power system network . The ILR and ANN RMSE were 0.0021 and 0.0019 respectively.
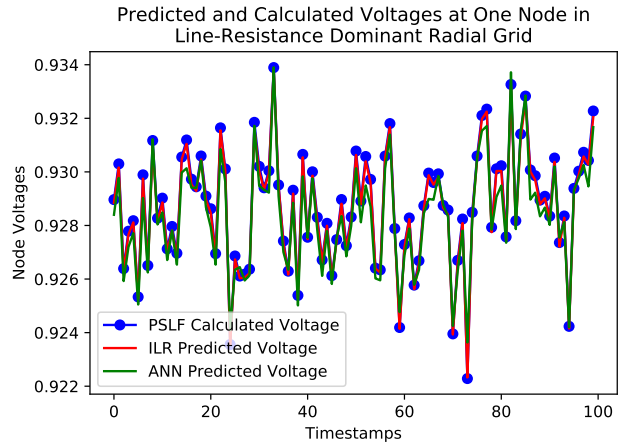

Fig. 10. Comparison of voltage profiles: PSLF calculated, ILR approximated and ANN approximated. Radial network included 500 houses

V. Conclusions

In this paper, multiple function approximation techniques are applied to a PSLF equation. The identity linear regression outperformed the ANN-based nonlinear regression which was contrary to the original hypothesis. More hyperparameter

tuning shows promise that the ANN RMSE can be reduce by 2 or 3 orders of magnitude, which would make it outperform the ILR solution as expected. Consideration of the extremums in the feature space moment could lead to an analytical selection of ANN hyperparameters. Further studies should include other features common to power system topologies found in Table. I.

REFERENCES

[1] F. Hayashi, *Econometrics*. Princeton University Press, 2000.

[2] I. Mann, "An Investigation of Nonlinear Speech Synthesis and Pitch Modification Techniques," Ph.D. dissertation, The University of Edinburgh, 1999.

[3] D. S. Chen and R. C. Jain, "A robust backpropagation learning algorithm for function approximation," *IEEE Transactions on Neural Networks*, vol. 5, no. 3, pp. 467–479, May 1994.

[4] D. Zhang and A. Benveniste, "Wavelet Networks," *IEEE Trans. Neural Networks*, 1992.

[5] D. Lowe, "On the Statistical Inversion of RBF Networks: a Statistical Interpretation," in *Second IEE International Conference on Artificial Neural Networks*, 1991.

[6] J. H. Friedman and W. Stuetzle, "Projection Pursuit Regression," *Journal of American Statistical Association*, 1981.

[7] X. M. Zhang, Y. Q. Chen, N. Ansari, and Y. Q. Shi, "Mini-max initialization for function approximation," *Neurocomputing*, vol. 57, pp. 389 – 409, 2004, new Aspects in Neurocomputing: 10th European Symposium on Artificial Neural Networks 2002. [Online]. Available: http://www.sciencedirect.com/science/article/pii/S0925231203005228

[8] B. Cheng and D. M. Titterington, "Neural Networks: A Review from Statistical Perspective," *Statistical Science*, vol. 9, no. 1, pp. 2–30, Feb. 1994.

[9] A. Barron, "[Neural Networks: A Review from Statistical Perspective]: Comment," *Statistical Science*, vol. 9, no. 1, pp. 2–30, Feb. 1994.

[10] J. Bergstra and Y. Bengio, "Random search for hyper-parameter optimization," *Journal of Machine Learning Research*, vol. 13, no. Feb, pp. 281–305, 2012.

[11] K. Du and M. Swamy, *Neural Networks and Statistical Learning*. Springer, London, 2014.